

[6] Spatial selectivity of the four-wave radiation converter in a transparent two-component medium in a scheme with concurrent pump waves



V.V. Ivakhnik[†], M.V. Savelyev[†]

[†]Samara National Research University, Samara, Russia

Abstract

Spatial characteristics of the degenerate four-wave radiation converter in a liquid containing nanoparticles were studied using a scheme with concurrent pump waves. The phase matching condition was shown to determine the general form of the spatial spectrum amplitude of the object wave, with the electrostriction phenomenon and Dufour effect shown to cause the emergence of dips in the spatial spectrum amplitude, with the dip positions corresponding to the propagation directions of the pump waves.

The relationship between characteristics of the dips and the pump wave parameters were obtained.

Keywords: SPATIAL SELECTIVITY, FOUR-WAVE RADIATION CONVERTER, TRANSPARENT TWO-COMPONENT MEDIUM.

Citation: IVAKHNIK VV, SAVELYEV MV. SPATIAL SELECTIVITY OF THE FOUR-WAVE RADIATION CONVERTER IN A TRANSPARENT TWO-COMPONENT MEDIUM IN A SCHEME WITH CONCURRENT PUMP WAVES. *COMPUTER OPTICS*, 2016; 40(3): 322-330. DOI: 10.18287/2412-6179-2016-40-3-322-330.

Introduction

To generate phase conjugate (PC) wave in four-wave mixing two schemes are used: scheme with opposing pump waves and scheme with concurrent pump waves [1, 2]. The choice of first or second scheme depends on the problem being solved and requirements imposed on the PC wave. In four-wave mixing in scheme with opposing pump waves PC of the incident (signal) wave is complete. The PC wave (object wave) propagates towards the signal wave and when it passes again through the same optically inhomogeneous medium through which the signal wave passed the phase distortions introduced into the signal wave are compensated [3].

In the scheme with concurrent pump waves only the transverse component of the wave vector of the incident wave is reversed. The PC wave propagates in the direction of the signal wave. It may be preferable, for example, to compensate for phase distortions arising when the signal wave propagates through one optically inhomogeneous medium and the PC wave propagates through another optically inhomogeneous medium the parameters of which are same or close to the parameters of the first medium [4].

Both four-wave mixing schemes with opposing and concurrent pump waves are used for image processing and analysis, in quantum cryptography, for ultra-high-speed optical signal processing, etc. [5–7].

Up to present time, the PC quality analysis has been carried out for four-wave radiation converters with concurrent pump waves in the medium with Kerr, resonance, thermal nonlinearities [8–10]. In recent years, the possibility of using media containing particles of micro- and nanosize (colloidal solutions, suspensions, etc.) for realization of four-wave mixing has been actively discussed [11–16]. When liquids containing nanoparticles are used as nonlinear media a significant influence on the spatial structure of the PC wave can be provided by such physical processes as electrostriction and Dufour effect [17–19]. In this paper, we analyze spatial selectivity of the four-wave radiation converter with concurrent pump waves in the transparent liquid filled with nanoparticles the density of which is equal to the density of liquid.

1. Four-wave mixing model

We consider the typical scheme of degenerate four-wave mixing $\omega+\omega-\omega=\omega$ with concurrent pump waves in a plane layer thickness ℓ (fig. 1).

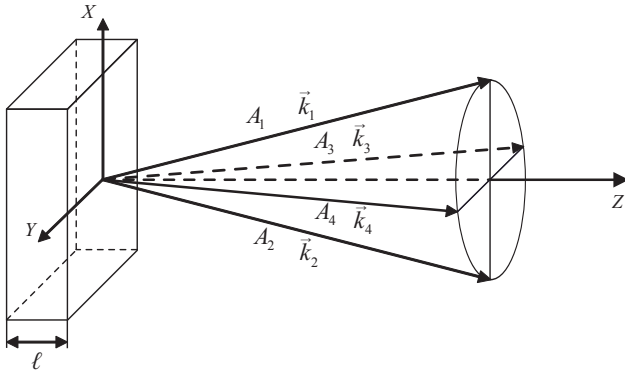


Fig. 1. Four-wave mixing scheme with concurrent pump waves

In the medium two plane pump waves with complex amplitudes $A_{1,2}(\vec{r}) = \tilde{A}_{1,2}(z) \exp(-i\vec{k}_{1,2}\vec{r})$ ($\vec{k}_{1,2}(\vec{\kappa}_{1,2}, k_{1,2z})$ are the wave vectors of the pump waves, z is the longitudinal component of the radius vector \vec{r}) propagate and the signal wave with complex amplitude A_3 propagates. We assume that the wave vectors of the pump waves lie in the XZ-plane (the plane of the pump waves). Interference of the pump waves and the signal wave leads to a change in the radiation intensity in space and, due to electrostriction, to the emergence of the nanoparticles concentration flux. Due to Dufour effect the concentration flux changes the temperature (δT), and hence the refractive index of the medium ($\delta n = (dn/dT)\delta T$). As a result of diffraction of the pump waves on the refractive index gratings, the object wave with complex amplitude A_4 is generated.

The initial Helmholtz equation describing four-wave mixing of radiation in the transparent nonlinear medium has the form [17, 18]

$$\left(\nabla^2 + k^2 + \frac{2k^2}{n_0} \frac{dn}{dT} \delta T \right) (A + A^*) = 0 \tag{1}$$

where $A = \sum_{j=1}^4 A_j$, $k = \omega n_0 / c$, ω is the cyclic frequency, n_0 is the average value of the refractive index, c is the speed of light.

Equation (1) is supplemented by a system of material equations for the concentration (δC) and temperature variation [11, 19]

$$\frac{\partial \delta C}{\partial t} = D_{22} \nabla^2 \delta C + \gamma \nabla^2 I, \tag{2}$$

$$c_p \nu \frac{\partial \delta T}{\partial t} = D_{11} \nabla^2 \delta T + D_{12} \nabla^2 \delta C. \tag{3}$$

Here, D_{11} , D_{22} , D_{12} and γ are the coefficients of thermal conductivity, diffusion, Dufour and electrostriction respectively, c_p is the specific heat of matter, ν is the density of matter, $I = AA^*$ is the intensity of radiation.

2. Four-wave mixing considering the temperature gratings arising from interference of the pump waves and the signal wave

For steady-state (stationary) regime, from the system of material equations (2) – (3) we obtain equation relating the temperature variation to the intensity of the interacting waves

$$\nabla^2 \delta T = \frac{\gamma D_{12}}{D_{11} D_{22}} \nabla^2 I. \tag{4}$$

In the pump waves approximation ($|A_{1,2}| \gg |A_{3,4}|$) with a small conversion coefficient ($|A_{1,2}| \gg |A_{3,4}|$) the intensity of radiation propagating in the nonlinear medium can be written as follows

$$I = I_0 + A_1 A_3^* + A_1^* A_3 + A_2 A_3^* + A_2^* A_3, \tag{5}$$

where $I_0 = I_1 + I_2$, $I_{1,2} = A_{1,2} A_{1,2}^*$.

Then the temperature variation can be represented as a sum of rapidly (δT_{31} , δT_{32}) and slowly (δT_0) varying components depending on the coordinates

$$\delta T(\vec{r}) = \delta T_0(z) + \delta T_{31}(\vec{r}) + \delta T_{31}^*(\vec{r}) + \delta T_{32}(\vec{r}) + \delta T_{32}^*(\vec{r}). \tag{6}$$

We expand the signal and object waves into plane waves and the rapidly varying components of the temperature variation into harmonic gratings

$$A_j(\vec{r}) = \int_{-\infty}^{\infty} \tilde{A}_j(\vec{\kappa}_j, z) \exp(-i\vec{\kappa}_j \vec{\rho} - ik_{jz} z) d\vec{\kappa}_j, \tag{7}$$

$$\delta T_{31,2}(\vec{r}) = \int_{-\infty}^{\infty} \delta \tilde{T}_{31,2}(\vec{\kappa}_{T1,2}, z) \exp(-i\vec{\kappa}_{T1,2} \vec{\rho}) d\vec{\kappa}_{T1,2}. \tag{8}$$

Here, \tilde{A}_j is the spatial spectrum of the j th wave, $\delta \tilde{T}_{31,2}$ are the spatial spectra of the temperature gratings, $\vec{\kappa}_j(\kappa_{jx}, \kappa_{jy})$ and k_{jz} are the transverse and longitudinal components of the wave vector \vec{k}_j , $j=3,4$, $|\vec{k}_j| = k$, $\vec{\kappa}_{T1,2}(\kappa_{T1,2x}, \kappa_{T1,2y})$ are the wave vectors of the temperature gratings, $\vec{\rho}(x, y)$ is the transverse component of the radius vector.

As shown in [9, 10], when the boundary condition $\tilde{A}_4(\vec{\kappa}_4, z=0) = 0$ is performed and only the temperature gratings are recorded in the nonlinear medium the spatial spectrum of the object wave on the back edge of the nonlinear layer is related to the spectra of the temperature gratings by the following expression

$$\begin{aligned} \tilde{A}'_4(\vec{\kappa}_4, z=\ell) = & -i \frac{k}{n_0} \frac{dn}{dT} \tilde{A}_{20} \times \\ & \times \int_0^\ell \delta \tilde{T}_{31}(\vec{\kappa}_{T1}, z) \exp[-i(k_{2z} - k_{4z})z] dz - \\ & -i \frac{k}{n_0} \frac{dn}{dT} \tilde{A}_{10} \int_0^\ell \delta \tilde{T}_{32}(\vec{\kappa}_{T2}, z) \exp[-i(k_{1z} - k_{4z})z] dz. \end{aligned} \tag{9}$$

Here, $\tilde{A}'_4(\vec{\kappa}_4, z) = \tilde{A}_4(\vec{\kappa}_4, z) \exp[P(z)]$,

$$P(z) = i \frac{k}{n_0} \frac{dn}{dT} \int_0^z \delta T_0(z_1) dz_1, \quad \tilde{A}_{1,20} = \tilde{A}_{1,2}(z=0).$$

Expression (9) is written for quasicollinear propagation of the interacting waves under condition

$$\vec{\kappa}_4 = \vec{\kappa}_{T1} + \vec{\kappa}_2 = \vec{\kappa}_{T2} + \vec{\kappa}_1.$$

Expression for the spatial spectrum of the object wave is supplemented by a system of differential equations derived from the material equation (4) describing the change in spatial spectra of the temperature gratings along the thickness of the nonlinear layer

$$\left(\frac{d^2}{dz^2} - \kappa_{T1,2}^2\right) \delta\tilde{T}_{31,2}(\vec{\kappa}_{T1,2}, z) = -\gamma \frac{D_{12}}{D_{11}D_{22}} \tilde{A}_{1,20} \tilde{A}_{30}^*(\vec{\kappa}_3) \times \quad (10)$$

$$\times \left[\kappa_{T1,2}^2 + (k_{1,2z} - k_{3z})^2 \right] \exp[-i(k_{1,2z} - k_{3z})z]$$

where $\tilde{A}_{30}(\vec{\kappa}_3) = \tilde{A}_{30}(\vec{\kappa}_3, z=0)$, $\vec{\kappa}_{T1,2} = \vec{\kappa}_{1,2} - \vec{\kappa}_3$.

If the temperature is constant on the edges of the nonlinear layer ($\delta\tilde{T}_{31,2}(\vec{\kappa}_{T1,2}, z=0) = \delta\tilde{T}_{31,2}(\vec{\kappa}_{T1,2}, z=\ell) = 0$) the solutions of equations (10) are

$$\delta\tilde{T}_{31,2}(\vec{\kappa}_{T1,2}, z) = \frac{\gamma D_{12} \tilde{A}_{1,20} \tilde{A}_{30}^*(\vec{\kappa}_3)}{D_{11} D_{22}} \left(\sinh^{-1}(\kappa_{T1,2} \ell) \times \right. \quad (11)$$

$$\times \left\{ \exp[-i(k_{1,2z} - k_{3z})\ell] \sinh(\kappa_{T1,2} z) - \right.$$

$$\left. \left. - \sinh[\kappa_{T1,2}(z - \ell)] \right\} - \exp[-i(k_{1,2z} - k_{3z})z] \right).$$

Substituting (11) into (9) and integrating over the z coordinate we obtain the spatial spectrum of the object wave on the back edge of the nonlinear medium

$$\tilde{A}'_4(\vec{\kappa}_4, z = \ell) = \tilde{A}'_{41}(\vec{\kappa}_4, z = \ell) + \tilde{A}'_{42}(\vec{\kappa}_4, z = \ell). \quad (12)$$

Here,

$$\tilde{A}'_{41,2}(\vec{\kappa}_4, z = \ell) = -i \frac{k\gamma D_{12}}{n_0 D_{11} D_{22}} \frac{dn}{dT} \times \quad (13)$$

$$\times \tilde{A}_{10} \tilde{A}_{20} \tilde{A}_{30}^*(\vec{\kappa}_3) \left[(2 \sinh(\kappa_{T1,2} \ell))^{-1} \times \right.$$

$$\times \left\{ \exp[-i(k_{1,2z} - k_{3z})\ell] - \exp(-\kappa_{T1,2} \ell) \right\} \times$$

$$\times \frac{\exp\left\{ [\kappa_{T1,2} - i(k_{2,1z} - k_{4z})]\ell \right\} - 1}{\kappa_{T1,2} - i(k_{2,1z} - k_{4z})} +$$

$$\left. + \left\{ \exp[-i(k_{1,2z} - k_{3z})\ell] - \exp(\kappa_{T1,2} \ell) \right\} \times \right.$$

$$\times \left. \frac{\exp\left\{ -[\kappa_{T1,2} + i(k_{2,1z} - k_{4z})]\ell \right\} - 1}{\kappa_{T1,2} + i(k_{2,1z} - k_{4z})} \right) -$$

$$-i \Delta^{-1} \left[\exp(-i\Delta \ell) - 1 \right],$$

$\Delta = (\vec{\kappa}_1 + \vec{\kappa}_2 - \vec{\kappa}_3 - \vec{\kappa}_4)$ is the projection of the wave mismatch on the Z-axis, $\kappa_{T1,2} = |\vec{\kappa}_{T1,2}|$. In the paraxial approximation $\Delta = (\vec{\kappa}_1 - \vec{\kappa}_4)(\vec{\kappa}_2 - \vec{\kappa}_4)/k$.

The spatial spectrum of the object wave is the sum of the spatial spectra of two waves one of which arises when the first pump wave diffracts on the tempera-

ture grating $\delta\tilde{T}_{32}$ and the other arises when the second pump wave diffracts on the temperature grating $\delta\tilde{T}_{31}$. If one of the pump waves, for example A_2 , is incoherent with the first pump wave and the signal wave then one temperature grating $\delta\tilde{T}_{31}$ is recorded in the nonlinear medium, and the spatial spectrum of the object wave is determined by the spatial spectrum of the wave \tilde{A}'_{41} . In this and the following section we'll assume that the signal wave is a wave from a point source located on the front edge of the nonlinear medium ($\tilde{A}_{30}(\vec{\kappa}_3) = 1$). In fig. 1 the characteristic modules of the spatial spectrum of the object wave are added in the presence of one (fig. 2a) and two (fig. 2b) temperature gratings provided that the pump waves fall on the nonlinear medium at the equal angles ($\vec{\kappa}_1 = -\vec{\kappa}_2$). Dependence of the projection of the wave mismatch on the Z-axis on the transverse components of the wave vectors of the interacting waves (the phase-matching condition) determines the general form of the spatial spectrum module of the object wave [8], and the presence of electrostriction and Dufour effect determines the emergence of the dips in the spectrum module the positions of which correspond to the directions of the pump waves propagation.

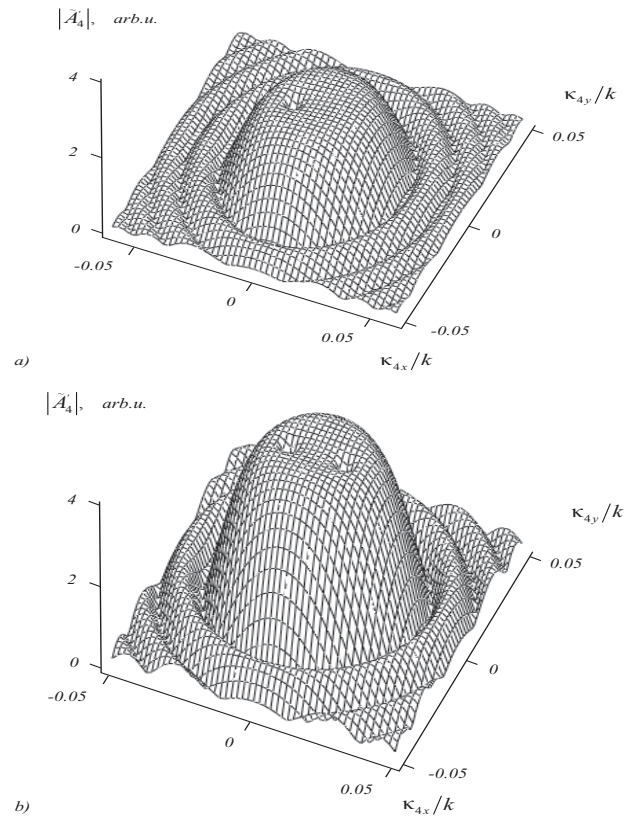


Fig. 2. Spatial spectra of the object wave with considering one (a) and two (b) temperature gratings at $k\ell = 5000$, $\kappa_{1x}/k = -\kappa_{2x}/k = 0.01$

When one temperature grating $\delta\tilde{T}_{31}$ is recorded and only phase-matching condition is considered in the plane of the pump waves ($(\bar{\kappa}_4, \bar{\kappa}_2) = \kappa_4, \kappa_2$) two maxima are observed in the spatial spectrum of the object wave, the positions of which are defined by the spatial frequencies of the pump waves $\kappa_{1,2} = |\bar{\kappa}_{1,2}|$.

As follows from (11) considering, in addition to the phase-matching condition, the electrostriction phenomenon and Dufour effect leads to the absence of the temperature grating at $\kappa_{T1} \rightarrow 0$ and to the emergence of the dip instead maximum in the spatial spectrum module of the object wave at the spatial frequency of the second pump wave (fig. 3a). At the fixed incidence angle of the first pump wave the rotation of the second pump wave shifts the dip position in the spatial spectrum by the amount of rotation.

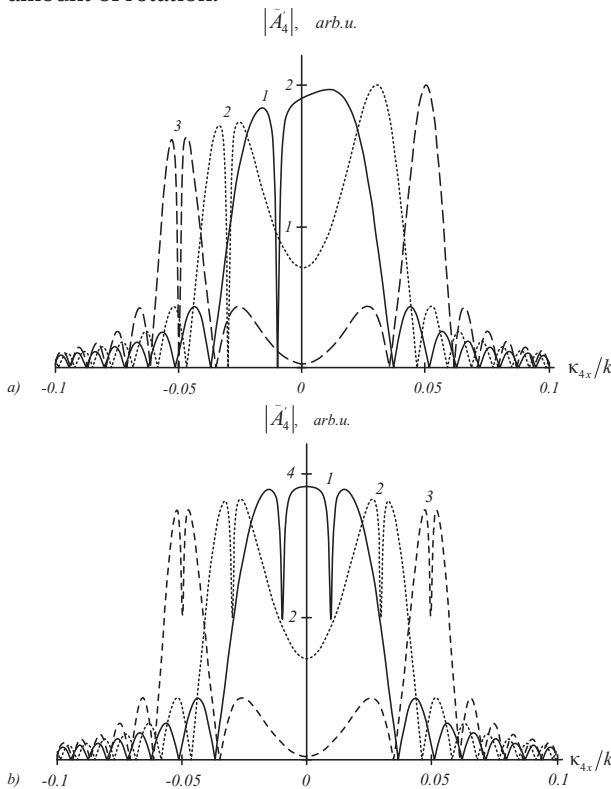


Fig. 3. Spatial spectra of the object wave in the plane of the pump waves with considering one (a) and two (b) temperature gratings at $k\ell = 5000$, $\kappa_{1x}/k = -\kappa_{2x}/k = 0.01$ (1), 0.03 (2), 0.05 (3)

The propagation direction of the pump waves doesn't influence the spatial spectrum module of the object wave in the dip area.

When two temperature gratings are recorded in the plane of the pump waves two dips are observed in the spatial spectrum module of the object wave, the positions of which are determined by the spatial frequencies of the pump waves (fig. 3b). In contrast with

recording of one temperature grating when the minimum value of the spatial spectrum module is zero in the dip, when two gratings are recorded the minimum value of the spatial spectrum module is not zero in the dip and it depends on the incidence angle of the pump waves on the nonlinear medium. The nonzero value of the spatial spectrum module in the dip is related to the recording of two temperature gratings in the medium. Thus, at the dip point ($\bar{\kappa}_4 = \bar{\kappa}_1$) the maximum value of the spatial spectrum of the object wave $\tilde{A}'_{42}(\bar{\kappa}_4, z = \ell)$ is superimposed on the zero value of the spatial spectrum of the object wave $\tilde{A}'_{41}(\bar{\kappa}_4, z = \ell)$.

We introduce a parameter characterizing the visibility of the dip in the spatial spectrum module of the object wave

$$V = \frac{A_{4\max} - A_{4\min}}{A_{4\max} + A_{4\min}} \quad (14)$$

where $A_{4\min} = |\tilde{A}'_4(\bar{\kappa}_4 = \bar{\kappa}_1, z = \ell)|$ is the value of the spatial spectrum module in the dip (on the spatial frequency of the first pump wave), $A_{4\max} = |\tilde{A}'_4(\bar{\kappa}_{4\max}, z = \ell)|$ is the largest value of the spatial spectrum module in the dip area under the condition $\kappa_{4\max} > \kappa_1$, $\kappa_{4\max} = |\bar{\kappa}_{4\max}|$ is the spatial frequency at which the largest value of the spatial spectrum is achieved.

To analyze the spatial selectivity of the four-wave radiation converter in the plane of the pump waves we introduce the dip width ($\Delta\kappa$)

$$\Delta\kappa = |\kappa_{41x} - \kappa_{42x}| \quad (15)$$

where κ_{41x} and κ_{42x} are the spatial frequencies in the dip area which are found from the solution of equation

$$|\tilde{A}'_4(\kappa_{41,2x}, \kappa_{41,2y} = 0, z = \ell)| = \frac{A_{4\max} + A_{4\min}}{2} \quad (16)$$

When the pump waves fall on the nonlinear medium at the equal angles, the increase of the incidence angle leads to a monotonic decrease of the value $A_{4\max}$. The visibility (fig. 4, curve 1) and the dip width in the spatial spectrum module of the object wave (fig. 4, curve 2) is decreased.

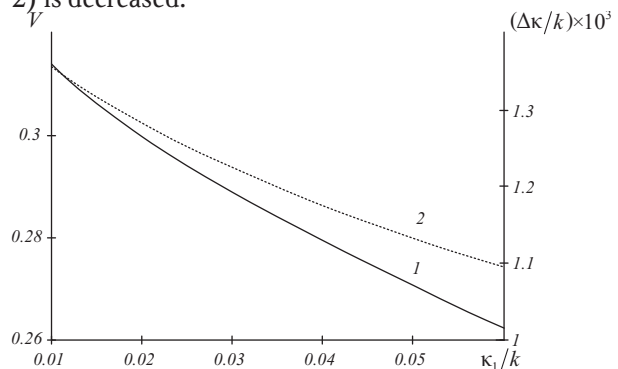


Fig. 4. Dependencies of the visibility (1) and the dip width (2) on the rotation angle of the pump waves at $k\ell = 5000$

The change of the spatial spectrum phase of the object wave (φ) considering both one and two temperature gratings are determined by the projection of the wave mismatch on the Z-axis and at $\bar{\kappa}_1 = -\bar{\kappa}_2$ is described well by a parabolic law

$$\varphi(\bar{\kappa}_4) = \frac{\ell}{2k} (\kappa_1^2 - \kappa_4^2). \tag{17}$$

3. Time evolution of the spatial spectrum of the object wave

In the case of nonstationary four-wave mixing the temporal dynamics of the particle concentration gratings influence significantly on the time dependence of the spatial spectrum of the object wave [19].

Like the temperature variation we represent the concentration variation as a sum of rapidly ($\delta C_{31}, \delta C_{32}$) and slowly (δC_0) varying components depending on the coordinates

$$\delta C(\vec{r}, t) = \delta C_0(z, t) + \delta C_{31}(\vec{r}, t) + \delta C_{31}^*(\vec{r}, t) + \delta C_{32}(\vec{r}, t) + \delta C_{32}^*(\vec{r}, t). \tag{18}$$

We expand the rapidly varying components of the concentration into harmonic gratings

$$\delta C_{31,2}(\vec{r}, t) = \int_{-\infty}^{\infty} \delta \tilde{C}_{31,2}(\bar{\kappa}_{C1,2}, z, t) \times \exp(-i\bar{\kappa}_{C1,2}\vec{\rho}) d\bar{\kappa}_{C1,2}. \tag{19}$$

Here, $\delta \tilde{C}_{31,2}$ are the spatial spectra of the concentration gratings caused by interference of the signal wave and the pump waves, $\bar{\kappa}_{C1,2}(\kappa_{C1,2x}, \kappa_{C1,2y})$ are the wave vectors of these gratings.

We'll assume that the spectra of the temperature grating like the spectra of the concentration gratings change over time. Considering expansion of the temperature and concentration gratings into harmonic gratings the system of equation (2) – (3) can be rewritten as follows

$$\begin{aligned} \frac{\partial \delta \tilde{C}_{31,2}(\bar{\kappa}_{C1,2}, z, t)}{\partial t} = & D_{22} \left(\frac{d^2}{dz^2} - \kappa_{C1,2}^2 \right) \delta \tilde{C}_{31,2}(\bar{\kappa}_{C1,2}, z, t) - \\ & - \gamma \left[(k_{1,2z} - k_{3z})^2 + \kappa_{C1,2}^2 \right] \times \\ & \times \tilde{A}_{1,20}(t) \tilde{A}_{30}^*(\bar{\kappa}_3, t) \exp[-i(k_{1,2z} - k_{3z})z], \\ c_p v \frac{\partial \delta \tilde{T}_{31,2}(\bar{\kappa}_{T1,2}, z, t)}{\partial t} = & D_{11} \left(\frac{d^2}{dz^2} - \kappa_{T1,2}^2 \right) \delta \tilde{T}_{31,2}(\bar{\kappa}_{T1,2}, z, t) + \\ & + D_{12} \left(\frac{d^2}{dz^2} - \kappa_{C1,2}^2 \right) \delta \tilde{C}_{31,2}(\bar{\kappa}_{C1,2}, z, t). \end{aligned} \tag{20}$$

Equations (20) – (21) are written under the condition $\bar{\kappa}_{C1,2} = \bar{\kappa}_{T1,2}$.

We'll find the solution of the system of equation (20) – (21) in the form of Fourier series

$$\begin{aligned} \delta \tilde{C}_{31,2}(\bar{\kappa}_{C1,2}, z, t) = & \frac{1}{2} C_{01,2}(\bar{\kappa}_{C1,2}, t) + \\ & + \sum_{m=1}^{\infty} C_{m1,2}(\bar{\kappa}_{C1,2}, t) \cos \frac{\pi m}{\ell} z, \\ \delta \tilde{T}_{31,2}(\bar{\kappa}_{T1,2}, z, t) = & \sum_{s=1}^{\infty} T_{s1,2}(\bar{\kappa}_{T1,2}, t) \sin \frac{\pi s}{\ell} z \end{aligned} \tag{22}$$

where $C_{01,2}, C_{m1,2}, T_{s1,2}$ are the coefficients of series expansion.

Substituting (22) into the material equations (20) – (21) in the absence of the particle flux through the edges of the nonlinear layer $\left(\left. \frac{d\delta \tilde{C}_{31,2}}{dz} \right|_{z=0} = \left. \frac{d\delta \tilde{C}_{31,2}}{dz} \right|_{z=\ell} = 0 \right)$

with considering the initial conditions $\delta \tilde{C}_{31,2}(\bar{\kappa}_{C1,2}, z, t=0) = 0$ we find the coefficients $C_{01,2}, C_{m1,2}$. Knowing the expansion coefficients of the spectra of the concentration gratings in series with the temperature unchanged on the edges of the nonlinear layer, with considering the initial conditions $\delta \tilde{T}_{31,2}(\bar{\kappa}_{T1,2}, z, t=0) = 0$ we find the coefficients $T_{s1,2}$, and hence, time evolution of the spatial spectra of the temperature gratings in the form [19]

$$\begin{aligned} \delta \tilde{T}_{31,2}(\bar{\kappa}_{T1,2}, z, t) = & \frac{2i\gamma D_{12} \left[(k_{1,2z} - k_{3z})^2 + \kappa_{T1,2}^2 \right]}{c_p v \pi (k_{1,2z} - k_{3z}) \ell} \times \\ & \times \sum_{s=1}^{\infty} \sin \frac{\pi s}{\ell} z \int_0^t \exp \left\{ -\frac{D_{11}}{c_p v} \left[\left(\frac{\pi s}{\ell} \right)^2 + \kappa_{T1,2}^2 \right] (t - \tau) \right\} \times \\ & \times \left[\int_0^{\tau} \tilde{A}_{1,20}(\tau') \tilde{A}_{30}^*(\bar{\kappa}_3, \tau') \times \right. \\ & \times \left(\kappa_{T1,2}^2 \left\{ \exp[-i(k_{1,2z} - k_{3z})\ell] - 1 \right\} \left[1 - (-1)^s \right] s^{-1} \times \right. \\ & \times \exp[-D_{22} \kappa_{T1,2}^2 (\tau - \tau')] - \\ & \left. \left. - \sum_{m=1}^{\infty} \left\{ 1 - (-1)^m \exp[-i(k_{1,2z} - k_{3z})\ell] \right\} \times \right. \right. \\ & \times \left[\left(\frac{\pi m}{\ell} \right)^2 + \kappa_{T1,2}^2 \right] \left[1 - \left(\frac{\pi m}{(k_{1,2z} - k_{3z})\ell} \right)^2 \right]^{-1} \times \\ & \times \left[\frac{1 - (-1)^{s+m}}{s+m} + \frac{1 - (-1)^{s-m}}{s-m} \right] \times \\ & \left. \left. \times \exp \left\{ -D_{22} \left[\left(\frac{\pi m}{\ell} \right)^2 + \kappa_{T1,2}^2 \right] (\tau - \tau') \right\} \right] d\tau' \right] d\tau. \end{aligned} \tag{23}$$

For stationary recording regime of the temperature gratings ($t \rightarrow \infty$) expressions for $\delta \tilde{T}_{31,2}$ obtained from (23) coincide with expressions for the spatial spectra of the temperature gratings (11). Substituting (23) into (9), integrating over the z coordinate we obtain analytic expression for the time dependence of the spatial spectrum of the object wave as the sum of the spatial spectra of two waves

$$\begin{aligned}
 \tilde{A}'_{41,2}(\bar{\kappa}_4, t) = & \frac{-2\gamma D_{12} k \left[(k_{1,2z} - k_{3z})^2 + \kappa_{T1,2}^2 \right]}{c_p v n_0 (k_{1,2z} - k_{3z}) (k_{2,1z} - k_{4z})^2 \ell^2} \times \\
 & \times \frac{dn}{dT} \tilde{A}_{2,10}(t) \sum_{s=1}^{\infty} \left\{ 1 - (-1)^s \exp \left[-i(k_{2,1z} - k_{4z}) \ell \right] \right\} \times \\
 & \times \left[1 - \left(\frac{\pi s}{\ell (k_{2,1z} - k_{4z})} \right)^2 \right]^{-1} \times \\
 & \times \int_0^t \exp \left\{ -\frac{D_{11}}{c_p v} \left[\left(\frac{\pi s}{\ell} \right)^2 + \kappa_{T1,2}^2 \right] (t - \tau) \right\} \times \\
 & \times \int_0^{\tau} \tilde{A}_{1,20}(\tau') \tilde{A}_{30}^*(\bar{\kappa}_3, \tau') \times \\
 & \times \left(\kappa_{T1,2}^2 \left\{ \exp \left[-i(k_{1,2z} - k_{3z}) \ell \right] - 1 \right\} \right) \times \\
 & \times \left[1 - (-1)^s \right] \exp \left[-D_{22} \kappa_{T1,2}^2 (\tau - \tau') \right] - \\
 & - \sum_{m=1}^{\infty} \left[\left(\frac{\pi m}{\ell} \right)^2 + \kappa_{T1,2}^2 \right] \left[\frac{1 - (-1)^{s+m}}{s+m} + \frac{1 - (-1)^{s-m}}{s-m} \right] \times \\
 & \times \left\{ 1 - (-1)^m \exp \left[-i(k_{1,2z} - k_{3z}) \ell \right] \right\} \times \\
 & \times \left[1 - \left(\frac{\pi m}{\ell (k_{1,2z} - k_{3z})} \right)^2 \right]^{-1} \times \\
 & \times \exp \left\{ -D_{22} \left[\left(\frac{\pi m}{\ell} \right)^2 + \kappa_{T1,2}^2 \right] (\tau - \tau') \right\} \left. \right\} d\tau' \right] d\tau.
 \end{aligned} \tag{24}$$

Expressions (13) and (24) describing the spatial spectra of the object waves on the back edge of the nonlinear layer in the scheme with concurrent pump waves coincide formally with similar expressions for the spatial spectra of the degenerate and non-degenerate four-wave radiation converters on the front edge in the scheme with opposing pump waves [18, 19]. Expressions for the projection of the wave mismatch Δ and for the difference of the projections of the wave vectors of the interacting waves on the Z -axis change.

In fig. 5 temporal dynamics of the spatial spectrum of the object wave in the plane of the pump waves is represented under the condition that the amplitudes of the pump waves are unchanged over time ($\tilde{A}_{1,20}(t) = \text{const}$). Seen that the formation of the dips in the spatial spectrum module caused by the presence of electrostriction phenomenon and Dufour effect is delayed compared to the formation of the spatial spectrum module caused by the nonzero projection of the wave mismatch on the Z -axis. This is due to the dependence of the recording time of the temperature gratings on the spatial frequencies $\kappa_{T1,2}$. In the dip area two temperature gratings are recorded, the recording time of one of which is determined by the spatial frequency of the pump wave, and the recording time of the second temperature grating tends to "infinity". The addition of the spatial spectra of two object waves corresponding to these gratings leads to a delay in the formation of the dips.

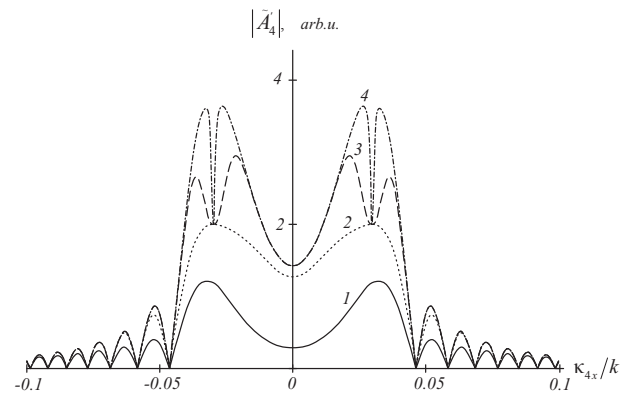


Fig. 5. Spatial spectra of the object wave at different time points in the plane of the pump waves with considering two temperature gratings at $k\ell = 5000$, $\kappa_{1x}/k = -\kappa_{2x}/k = 0.03$, $c_p v D_{22}/D_{11} = 2 \times 10^{-5}$, $t D_{22}/\ell^2 = 10^{-5}$ (1), 10^{-4} (2), 10^{-3} (3), 10^{-1} (4)

The visibility of the dip in the spatial spectrum module of the object wave increases over time reaching a steady-state value (fig. 6).

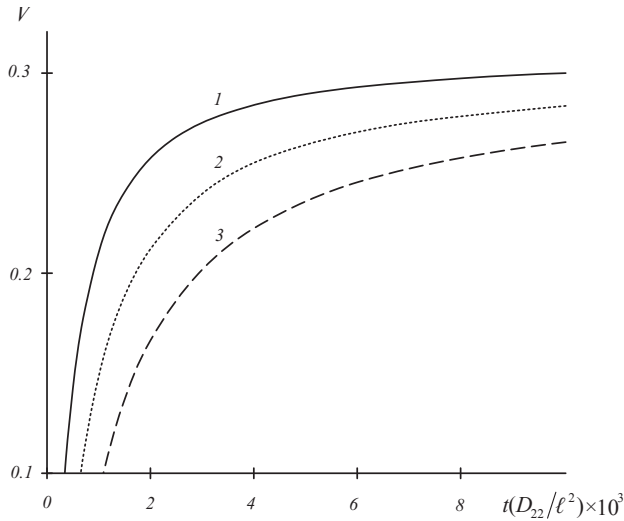


Fig. 6. Time dependence of the visibility of the dip at $k\ell = 5000$, $c_p \nu D_{22}/D_{11} = 2 \times 10^{-5}$, $\kappa_{1x}/k = -\kappa_{2x}/k = 0.01$ (1), 0.03 (2), 0.05 (3)

To characterize time dynamics of the dip we introduce the formation time of the dip (Δt) as the time during which the visibility reaches a value of 10% then with increasing of the incidence angle of the pump waves on the nonlinear medium the normalized formation time of the dip increases and for the incidence angles $\kappa_{1x}/k = -\kappa_{2x}/k = 0.02, 0.03, 0.04$ rad is $\Delta t D_{22}/\ell^2 = 3.445 \times 10^{-4}, 6.49 \times 10^{-4}, 1.077 \times 10^{-3}$ respectively.

The rate of the time change of the visibility of the dip in a range of values from 10 to 20% decreases with increasing of the incidence angle of the pump waves.

4. Four-wave mixing at large conversion coefficients

Let us consider stationary concurrent four-wave mixing in the transparent two-component medium considering the fact that the intensity of the object wave is comparable or even larger than the intensity of the signal wave (regime of the large conversion coefficients is realized). In this case it's necessary to consider the temperature gratings that arise when the object wave interferes with the pump waves.

In expressions for the intensity and the temperature variation (5) – (6) the terms $A_2 A_4^* + A_2^* A_4 + A_1 A_4^* + A_1^* A_4$, $\delta T_{42} + \delta T_{42}^* + \delta T_{41} + \delta T_{41}^*$ are added respectively.

The rapidly varying in space components of the temperature $\delta T_{42,1}(\vec{r})$, as well as $\delta T_{31,2}(\vec{r})$, we expand into harmonic gratings.

$$\delta T_{42,1}(\vec{r}) = \int_{-\infty}^{\infty} \delta \tilde{T}_{42,1}(\vec{\kappa}_{T3,4}, z) \times \exp(-i\vec{\kappa}_{T3,4}\vec{\rho}) d\vec{\kappa}_{T3,4}. \quad (25)$$

Here, $\delta \tilde{T}_{42,1}$ are the spatial spectra of the temperature gratings caused by interference of the object wave and the pump waves, $\vec{\kappa}_{T3,4}(\kappa_{T3,4x}, \kappa_{T3,4y})$ are the wave vectors of these gratings.

Equations describing changes in the spatial spectra of the signal and object waves and the spatial spectra of the temperature gratings under quasicollinear propagation of the interacting waves take the form

$$\frac{d\tilde{A}'_3}{dz} + i \frac{k}{n_0} \frac{dn}{dT} \left\{ (\delta \tilde{T}_{31}^* + \delta \tilde{T}_{42}) \tilde{A}_{10} \times \exp[-i(k_{1z} - k_{3z})z] + (\delta \tilde{T}_{32}^* + \delta \tilde{T}_{41}) \tilde{A}_{20} \times \exp[-i(k_{2z} - k_{3z})z] \right\} = 0, \quad (26)$$

$$\frac{d\tilde{A}'_4}{dz} + i \frac{k}{n_0} \frac{dn}{dT} \left\{ (\delta \tilde{T}_{31} + \delta \tilde{T}_{42}^*) \tilde{A}_{20} \times \exp[-i(k_{2z} - k_{4z})z] + (\delta \tilde{T}_{32} + \delta \tilde{T}_{41}^*) \tilde{A}_{10} \times \exp[-i(k_{1z} - k_{4z})z] \right\} = 0, \quad (27)$$

$$\left(\frac{d^2}{dz^2} - \kappa_{T1,2}^2 \right) \delta \tilde{T}_{31,2}(\vec{\kappa}_{T1,2}, z) = -\frac{\gamma D_{12}}{D_{11} D_{22}} \tilde{A}_{1,20} \times \exp[-i(k_{1,2z} - k_{3z})z] \left[2i(k_{1,2z} - k_{3z}) \frac{d}{dz} + \kappa_{T1,2}^2 + (k_{1,2z} - k_{3z})^2 \right] \tilde{A}'_3(\vec{\kappa}_3, z), \quad (28)$$

$$\left(\frac{d^2}{dz^2} - \kappa_{T3,4}^2 \right) \delta \tilde{T}_{42,1}(\vec{\kappa}_{T3,4}, z) = -\frac{\gamma D_{12}}{D_{11} D_{22}} \tilde{A}_{2,10} \times \exp[-i(k_{2,1z} - k_{4z})z] \left[2i(k_{2,1z} - k_{4z}) \frac{d}{dz} + \kappa_{T3,4}^2 + (k_{2,1z} - k_{4z})^2 \right] \tilde{A}'_4(\vec{\kappa}_4, z). \quad (29)$$

Here, $\tilde{A}'_3(\vec{\kappa}_3, z) = \tilde{A}_3(\vec{\kappa}_3, z) \exp[P(z)]$, $\kappa_{T3,4} = |\vec{\kappa}_{T3,4}| = |\vec{\kappa}_{2,1} - \vec{\kappa}_4|$.

In fig. 7 the dependencies of the amplitude conversion coefficient $T = |A_{4\max}/\tilde{A}'_{30}|$ and the dip half-width ($\Delta \kappa_{1/2} = |\kappa_{41x} - \kappa_{1x}|$, $\kappa_{41x} > \kappa_{1x}$) on the normalized intensity of the pump waves ($G = k\gamma D_{12} (dn/dT) I_1/n_0 D_{11} D_{22}$) obtained by numerical analysis of the system of equations (26) – (29) are adduced at the equal intensities of the pump waves ($I_1 = I_2$). The increase in the intensity of the pump waves leads to a linear increase in the amplitude conversion coefficient while the dip half-width doesn't change within $\pm 4\%$. The accuracy of finding the dip half-

width has been determined by the error in calculating the position of the largest value of the spatial spectrum module. A similar character of the dependence of the amplitude conversion coefficient on the inten-

sity of the pump waves is observed for the four-wave radiation converter with concurrent pump waves on thermal nonlinearity [10].

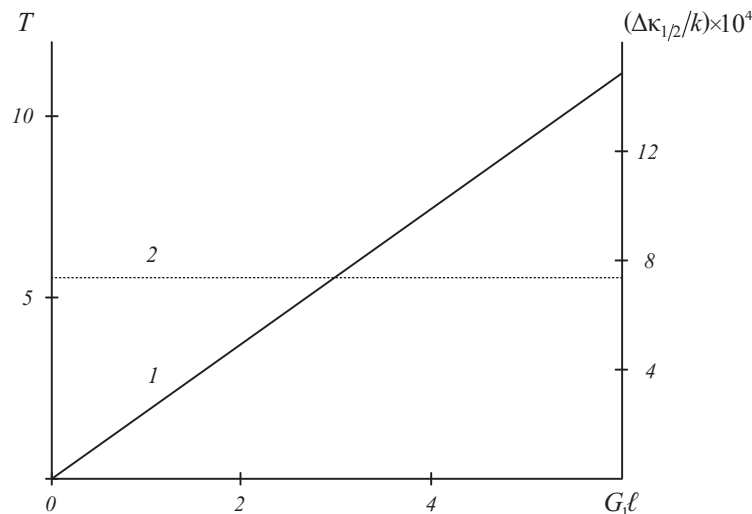


Fig. 7. Dependencies of the conversion coefficient (1) and the dip half-width (2) on the intensity of the first pump wave at $k\ell = 5000$, $\kappa_{1x}/k = -\kappa_{2x}/k = 10^{-3}$, $I_1 = I_2$

Conclusion

Analytical expressions that relate the spatial spectra of the object and signal waves are obtained for stationary and nonstationary regimes of degenerate four-wave mixing in the transparent two-component medium with concurrent pump waves with the small conversion coefficient. Established that the phase matching condition determines the general form of the spatial spectrum module of the object wave, and the presence of the electrostriction phenomenon and Dufour effect determines the emergence of the dips in the spatial spectrum module whose positions correspond to the propagation directions of the pump waves. The visibility of the dips increases over time reaching the steady-state value. With increasing of the incidence angle of the pump waves on the nonlinear medium the formation time of the dip increases and its visibility decreases.

The intensity grows of the pump waves at $I_1 = I_2$ leads to the increase in the amplitude conversion coefficient according to a linear law while the dip half-width is constant.

References

1. Zel'dovich BYa, Pilipetsky NF, Shkunov VV. Principles of phase conjugation. New York: Springer-Verlag Berlin Heidelberg; 1985. DOI: 10.1007/978-3-540-38959-0.
2. Dmitriev VG. Nonlinear optics and phase conjugation [In Russian]. Moscow: "Fizmatlit" Publisher; 2003.

3. Voronin ÉS, Petnikova VM, Shuvalov VV. Use of degenerate parametric processes for wavefront correction (review). Sov J Quantum Electron 1981; 8(5): 551-561. DOI: 10.1070/QE1981v-011n05ABEH006899.
4. Hellwarth RW. Optical beam phase conjugation four-wave mixing in a waveguide. Opt Eng 1982; 21(2): 263-265.
5. Ma X, Yang L, Guo X, Li X. Generation of photon pairs in dispersion shift fiber through spontaneous four wave mixing: Influence of self-phase modulation. Opt Commun 2011; 284(19): 4558-4562. DOI: 10.1016/j.optcom.2011.06.011.
6. Salem R, Foster MA, Turner AC, Geraghty DF, Lipson M, Gaeta AL. Optical time lens based on four-wave mixing on a silicon chip. Opt Lett 2008; 33(10): 1047-1049. DOI: 10.1364/OL.33.001047.
7. Scheulin AA, Angervaks AE, Ryskin AI. Holographic media based on crystals with fluorite structure with color centers [In Russian]. Saint-Petersburg: SPbSU ITMO Publisher; 2009.
8. Ivakhnik VV, Martasova ÉG, Nikonov VI. Quality of phase conjugation (PC) with prosperous four-photon interaction [In Russian]. Opt Spectrosc 1991; 70(1): 118-122.
9. Ivakhnik VV, Nikonov VI, Kharskaya TG. Analysis of spatial characteristics of the four-wave radiation converter on thermal nonlinearity in a scheme with concurrent pump waves [In Russian]. Computer Optics 2006; 30: 4-8.
10. Akimov AA, Ivakhnik VV, Nikonov VI. Four-wave interaction on resonance and thermal nonlinearities in a scheme with concurrent pump waves for high conversion coefficients. Radiophys Quantum Electron 2015; 57(8): 672-679. DOI: 10.1007/s11141-015-9553-x.

- **11.** Livashvili AI, Kostina GV, Yakunina MI. Temperature dynamics of a transparent nanoliquid acted on by a periodic light field. *J Opt Tech* 2013; 80(2): 124-126. DOI: 10.1364/JOT.80.000124.
- **12.** Rusconi R, Isa L, Piazza R. Thermal-lensing measurement of particle thermophoresis in aqueous dispersion. *J Opt Soc Am B* 2004; 21(3): 605-616. DOI: 10.1364/JOSAB.21.000605.
- **13.** Mahilny UV, Marmysh DN, Stankevich AI, Tolstik AL, Matusevich V, Kowarschik R. Holographic volume gratings in a glass-like polymer materials. *Appl Phys B* 2006; 82(2): 299-302. DOI: 10.1007/s00340-005-2006-z.
- **14.** Afanas'ev AA, Rubinov AN, Mikhnevich SYu, Ermolaev IE. Four-wave mixing in a liquid suspension of transparent dielectric microspheres. *JETP* 2005; 101(3): 389-400.
- **15.** Lopez-Mariscal C, Gutierrez-Vega JC, McGloin D, Dholaria K. Direct detection of optical phase conjugation in a colloidal medium. *Opt Express* 2007; 15(10): 6330-6335. DOI: 10.1364/OE.15.006330.
- **16.** El-Ganainy R, Christodoulides DN, Rotschild C, Segev M. Soliton dynamics and self-induced transparency in nonlinear nanosuspensions. *Opt Express* 2007; 15(16): 10207-10218. DOI: 10.1364/OE.15.010207.
- **17.** Ivakhnik VV, Savelyev MV. Four-wave mixing in a transparent medium based on electrostriction and Dufour effect at large reflectance. *Phys Procedia* 2015; 73: 26-32. DOI: 10.1016/j.phpro.2015.09.117.
- **18.** Ivakhnik VV, Savelyev MV. The influence of the reflection coefficient on the spatial selectivity of a four-wave radiation converter in a transparent medium based on electrostriction and Dufour effect [In Russian]. *Computer Optics* 2015; 39(2): 197-203.
- **19.** Ivakhnik VV, Savelyev MV. Spatial and temporal characteristics of a nondegenerate four-wave radiation converter in a transparent medium based on electrostriction and Dufour effect [In Russian]. *Computer Optics* 2015; 39(4): 486-491. DOI: 10.18287/0134-2452-2015-39-4-486-491.

